ELSEVIER

Chemical Engineering Journal 140 (2008) 614–620

Chemical Engineering Journal

www.elsevier.com/locate/cej

Short communication

Diffusion of hydrocarbon mixtures in MFI zeolite: Influence of intersection blocking

R. Krishna*, J.M. van Baten

Van't Hoff Institute for Molecular Sciences, University of Amsterdam, Nieuwe Achtergracht 166, 1018 WV Amsterdam, The Netherlands

Received 30 October 2007; received in revised form 17 November 2007; accepted 19 November 2007

Abstract

Branched and cyclic hydrocarbons such as *iso*-butane, 2-methylpentane, 3-methylpentane, 2,2-dimethyl-butane and benzene are preferentially adsorbed at the intersections of the channels of MFI zeolite; they serve as bottlenecks for molecular traffic in mixtures with linear C1–C6 alkanes. Molecular dynamics simulations show that as the loadings of tardier *i*C4, 2MP, 3MP, 22DMB, and Bz is progressively increased to four molecules per unit cell the diffusivity of the more mobile linear alkane reduces nearly to zero. The reduction in the *n*-alkane diffusivity is quantitatively similar irrespective of the branched/cyclic hydrocarbon.

Keywords: MFI zeolite; Self-diffusivity; Hydrocarbon mixtures; Branched hydrocarbons; Cyclic hydrocarbons; Molecular dynamics; Adsorption

1. Introduction

MFI zeolite membranes offer considerable potential for separating hydrocarbon mixtures [1–8]. The separation selectivity is dictated both by the adsorption and diffusion characteristics of the individual species in the mixture. In MFI zeolite each component in the mixture is influenced by the co-adsorbed species [9]; almost invariably the more mobile species is slowed down due to the presence of tardier partners. PFG NMR studies of Förste et al. [10] found that the self-diffusivity of methane (C1), D_{C1}, is significantly reduced as the loading of the co-adsorbed benzene (Bz), q_{Bz}, increases. In MAS PFG NMR studies, Fernandez et al. [11] found that the self-diffusivity of *n*-butane (*n*C4), D_{nC4}, in mixtures with *iso*-butane (*i*C4) decreases by an order of magnitude as the loading of *i*C4, q_{iC4}, is increased from 0 to 2 molecules per unit cell. For *n*-hexane (*n*C6)–2-methylpentane (2MP), and *n*C6–3-methylpentane (3MP) mixtures experimental studies [12,13] show that the D_{nC6} is reduced significantly as the 2MP or 3MP loadings increase.

The major aim of the present communication is to demonstrate that the observed reduction in the diffusivity of the linear alkane in C1–Bz, *n*C4–*i*C4, and *n*C6–2MP mixtures is characteristic of a much wider variety of mixtures. We aim to show that the tardier branched or cyclic hydrocarbons reduce molecular traffic along the channels of MFI by blocking the intersections where they prefer to locate. Using molecular dynamics (MD), we determined the self-diffusivity of a linear C1–C6 alkane in a wide variety of mixtures: C1–*i*C4, ethane (C2)–iC4, propane (C3)–iC4, *n*C4–*i*C4, *n*C6–2MP, *n*C6–3MP, *n*C6–2,2-dimethylbutane (22DMB), *n*C6–Bz, C1–22DMB, C1–Bz, and C3–Bz. Besides MD simulations we performed Configurational-Bias Monte-Carlo (CBMC) simulations to determine the adsorption equilibrium for pure components and binary mixtures. The CBMC and MD simulation methodologies are described in Supplementary Information accompanying this publication, along with pure component, and mixture adsorption data, snapshots and detailed simulation results for diffusivities. A selection of these results is discussed below.

2. Simulations of adsorption

CBMC simulations of the adsorption isotherms for C1, C2, C3, *n*C4, *i*C4, *n*C6, 2MP, 3MP, 22DMB, and Bz in MFI at 300 K are shown in Fig. 1a–c. We note that branched and cyclic hydrocarbons such as *i*C4, 2MP, 3MP, and Bz show a strong inflection at a loading, $q = 4$ molecules per unit cell. These molecules prefer to locate at the intersections because of the extra "leg room"

* Corresponding author. Tel.: +31 20 5257007; fax: +31 20 5255604.
E-mail address: r.krishna@uva.nl (R. Krishna).

1385-8947/$ – see front matter © 2007 Elsevier B.V. All rights reserved.
doi:10.1016/j.cej.2007.11.026

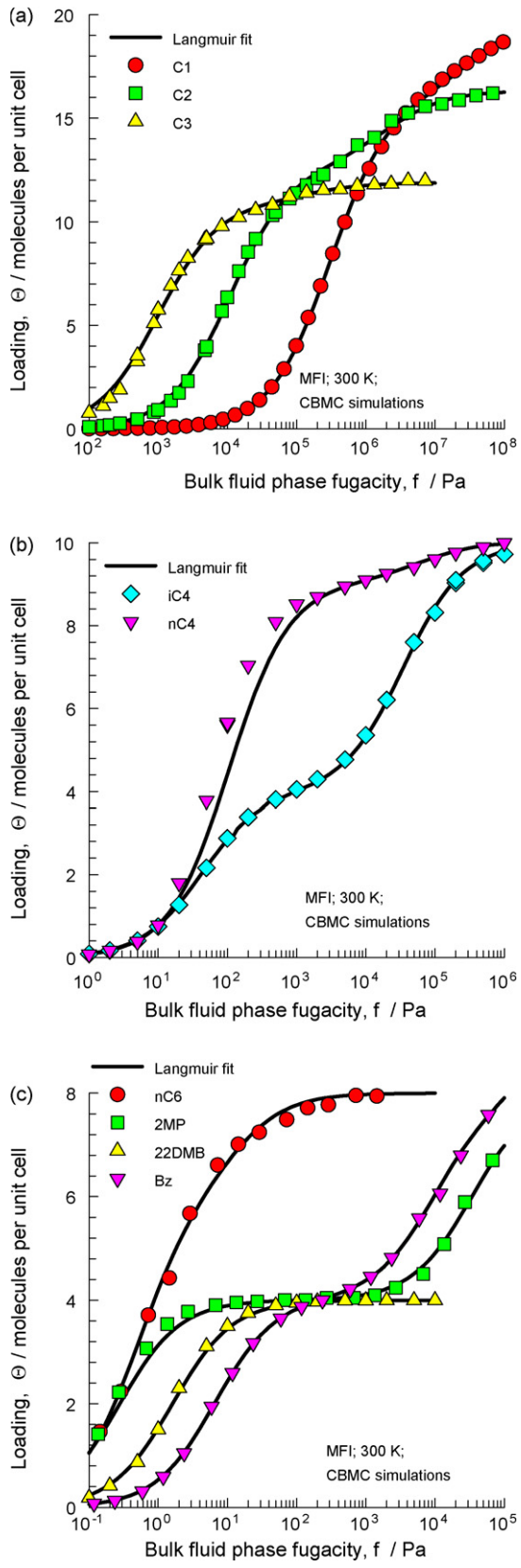

Fig. 1. CBMC simulations for pure component isotherms in MFI at 300 K for (a) C1, C2, C3, (b) *n*C4, *i*C4, (c) *n*C6, 2MP, 3MP, 22DMB, and Bz. The continuous solid lines represent 3-site Langmuir fits; the parameter values are given in Supplementary Information.

that is available here. An extra "push" is required to locate these molecules within the channel interiors; this extra push results in an inflection in the pure component isotherms at a loading of four molecules per unit cell [14–17]. For the compact and bulky 22DMB, the extra push is too large, and therefore $q = 4$ is also the saturation capacity.

The preferential location of *i*C4, 2MP, 3MP, 22DMB, and Bz at intersections also manifests for mixture adsorption, as illustrated in the snapshots in Fig. 2 for C3–*i*C4, C1–Bz, and *n*C6–22DMB mixtures. We see that *i*C4, Bz and 2MP are exclusively located at the intersections. The isotherm inflection has a significant influence on mixture adsorption, as illustrated for (a) *n*C4–*i*C4, (b) *n*C6–Bz, and (c) *n*C6–2MP mixtures in Fig. 3. The component loadings of *i*C4, Bz and 2MP all exhibit a maximum when the total mixture loading $q = 4$. For $q > 4$, the adsorption of the linear alkane is favored because it is more efficient to pack the channels of MFI with *linear* alkanes. The separation of hexane isomers by exploiting the differences in the packing efficiency of molecules has been stressed in earlier publications [16,18,19]; the same principle applies to other hydrocarbon mixtures. For all the mixtures investigated in this study, the multicomponent Langmuir model cannot be used to estimate the component loadings in the mixture because this model is unable to predict the maximum in the loading of the branched or cyclic hydrocarbon in the mixture. The Ideal Adsorbed Solution Theory (IAST) of Myers and Prausnitz [20], using only pure component isotherm data, is successful in providing a good *qualitative* representation of entropy effects during mixture sorption [21]. The IAST predictions are shown by the continuous solid lines in Fig. 3a–c. As can be seen from Fig. 3 the *quantitative* agreement between the predictions of IAST and CBMC mixture simulations are not perfect for the branched or cyclic hydrocarbon. This failure of the IAST to provide a good quantitative description of mixture adsorption has also been stressed earlier for C1–Bz, and C1–cyclohexane (CH) mixtures by Murthi and Snurr [22]. The reason for this imperfect prediction is to be found in *segregation* effects in mixture adsorption [22,23] found in a variety of zeolites.

For mixture loadings $q > 4$, the adsorption becomes increasingly segregated; the intersections sites will be occupied by the branched or cyclic hydrocarbons while the channels, straight and zig–zag, will have to accommodate increasing amount of the linear alkanes. The IAST assumes a homogenous adsorbed phase composition, and therefore its predictions of *i*C4, Bz and 2MP loadings will become increasingly poor for $q > 4$. For a good quantitative description of mixture adsorption, non-ideality effects caused by segregation have to be taken account of using the Real Adsorbed Solution Theory [24].

3. Simulations of diffusion

We carried out a set of simulations to determine the self-diffusivities a linear C1–C6 alkane in a variety of binary mixtures in which the loading of the branched or cyclic hydrocarbon was varied in the range 0–4 molecules per unit cell. The self-diffusivities of the branched or cyclic hydrocarbons are not reported because these molecules did not move sufficiently long

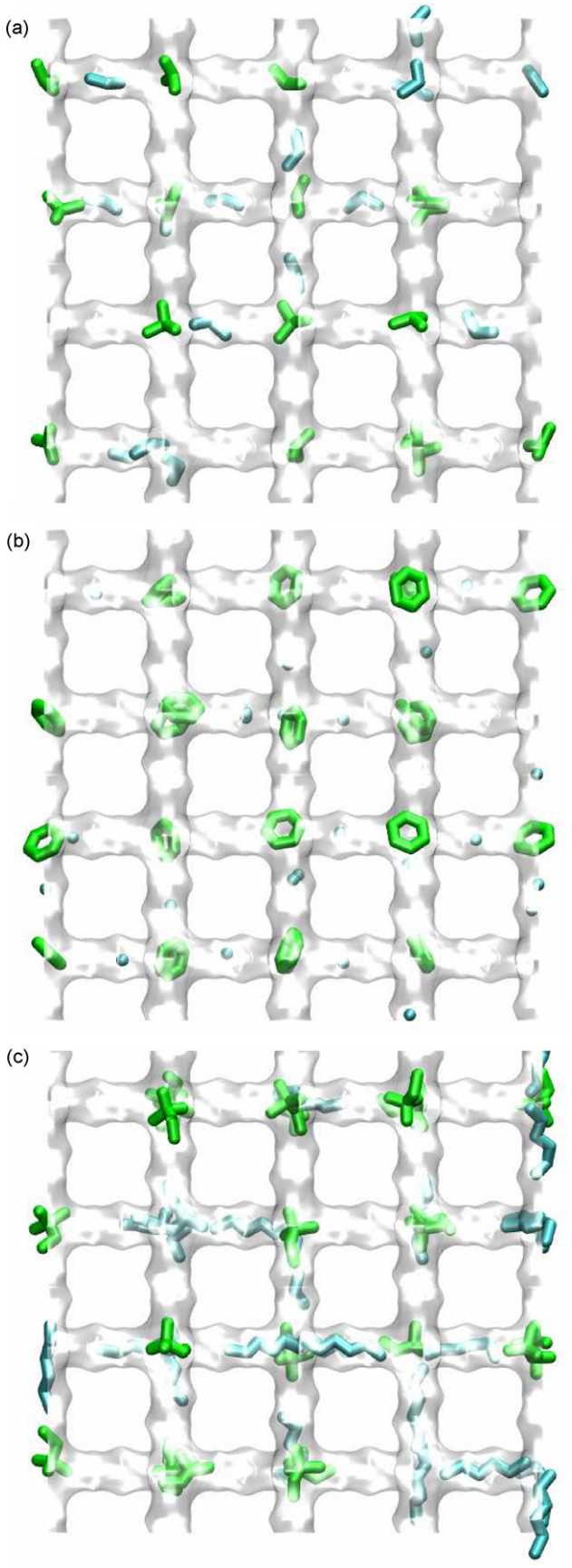

Fig. 2. Snapshots showing the location of (a) C3 and *i*C4, (b) C1 and Bz, and (c) *n*C6 and 22DMB, molecules in MFI, viewed from the side, in the *x*–*y* plane. The total loading $q = 4$, with equal loading of each species.

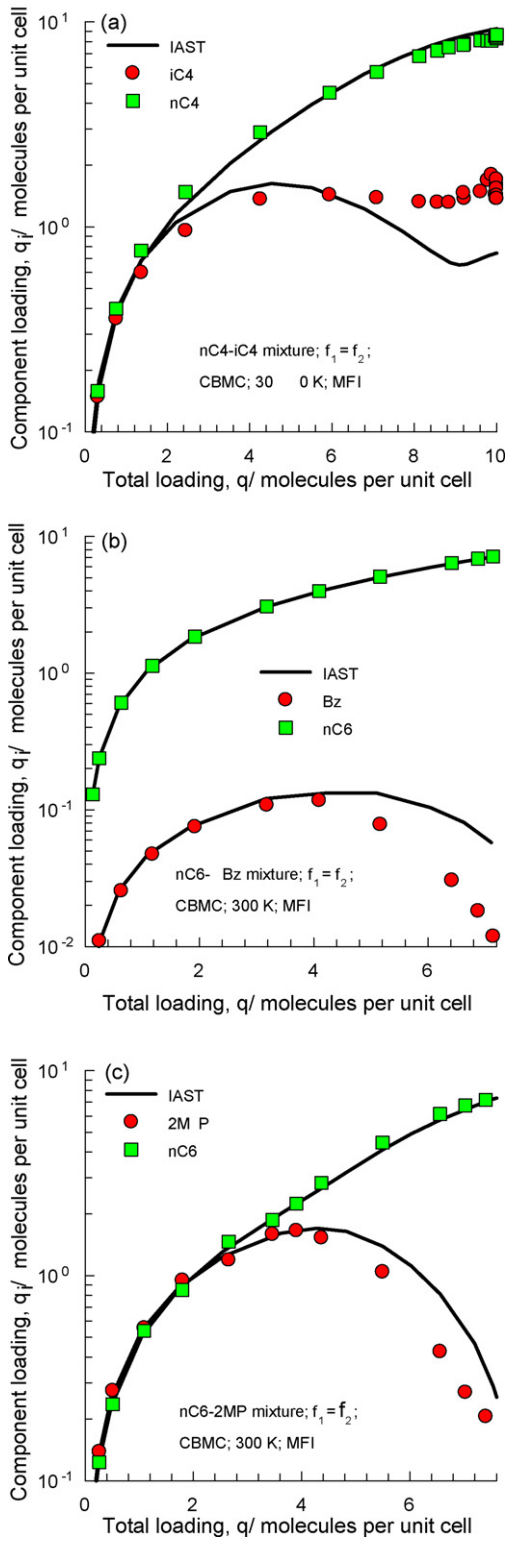

Fig. 3. CBMC simulations of the component loadings in (a) *n*C4–*i*C4, (b) *n*C6–Bz, and (c) *n*C6–2MP mixtures compared with the calculations of IAST, shown by the continuous solid lines.

distances during the simulation time in order to obtain reliable statistics required to calculate diffusivities.

Consider first diffusion in a mixture C1 and *i*C4 for which the total loading is maintained constant at $q = 4$. The self-diffusivity of C1 in *x*, *y*, and *z* directions of MFI are shown in Fig. 4a. The most prominent contribution is along the straight channels, in the *y*-direction. We note that $D_{C1,y}$ decreases practically linearly as q_{iC4} increases in value from 0 to 2. Fig. 4b and c present snapshots showing the location of C1 and *i*C4 for $q_{C1} = q_{iC4} = 2$; at this loading half the intersection sites are occupied by the extremely tardy *i*C4. Since the occupancy of the intersections is distributed randomly, each one of the straight channels has an *i*C4 molecule ensconced somewhere along the *y*-direction; see Fig. 4b and c. The occupation of *i*C4 at the intersections of the channels is tantamount to blockage, leading to severe reduction in the molecular traffic of the more mobile C1 along the straight channels. This explains the severe reduction in $D_{C1,y}$ at $q_{iC4} = 2$. For $q_{iC4} > 2$ the C1 molecules have to worm their way along the zig–zag channels in *x*- and *z*-directions, by-passing the blocked intersections. From Fig. 4a we note that for $q_{iC4} > 2$, $D_{C1,x} \approx D_{C1,y}$. An analogous picture emerges for each of the eleven binary mixtures investigated in the present study.

The orientation averaged diffusivity values for linear alkanes, $D = (D_x + D_y + D_z)/3$, are summarized in Fig. 5 as a function of the loading of its partner in various mixtures. From Fig. 5a we note that the dependence of D_{C1} on the loading of its partner, in mixtures with a constant total loading $q = 4$, is the same irrespective of its partner *i*C4, 22DMB, or Bz. We conclude that the blockage of the intersections by any one of *i*C4, 22DMB or Bz is *equally* deleterious to C1 traffic. The choice of total loading $q = 4$ in Fig. 5a is for illustration purposes; analogous results are obtained for $q > 4$.

Simulation results in which the loading of C1 in C1–Bz mixtures was maintained at $q_{C1} = 3$ are presented in Fig. 5b. The MD simulations are in excellent agreement with the results of Gupta and Snurr [25] who performed free energy perturbation calculations to determine D_{C1} in both C1–Bz and C1–CH mixtures; CH is ensconced at the intersections and reduces the traffic of C1 in same quantitative manner as *i*C4, 22DMB and Bz. The PFG NMR experiments of Förste et al. [10] for C1–Bz mixtures in ZSM-5 are also plotted in Fig. 5b for comparison; there is a good qualitative agreement between simulations and experiment.

The influence of increasing loading of *i*C4 on diffusion in C2–*i*C4 and *n*C4–*i*C4 mixtures is shown in Fig. 5c. The reduction of D_{C2} and D_{nC4} with q_{iC4} is similar; if the data were normalized with respect to pure linear alkane diffusivity, the results would fall on the same line. All normal alkanes experience a similar deleterious influence due to intersection blocking. Also plotted in Fig. 5c are the PFG NMR data of Fernandez et al. [11] for *n*C4–*i*C4 mixtures. The experiments show a sharp decline in D_{nC4} to virtually zero as q_{iC4} approaches 2; this decline is sharper than anticipated by MD simulations. The lack of perfect agreement between the MD simulations results for *n*C4–*i*C4 mixtures when compared to experimental data is due to the extreme sensitivity of MD simulations to very small alterations in the chosen force field [26].

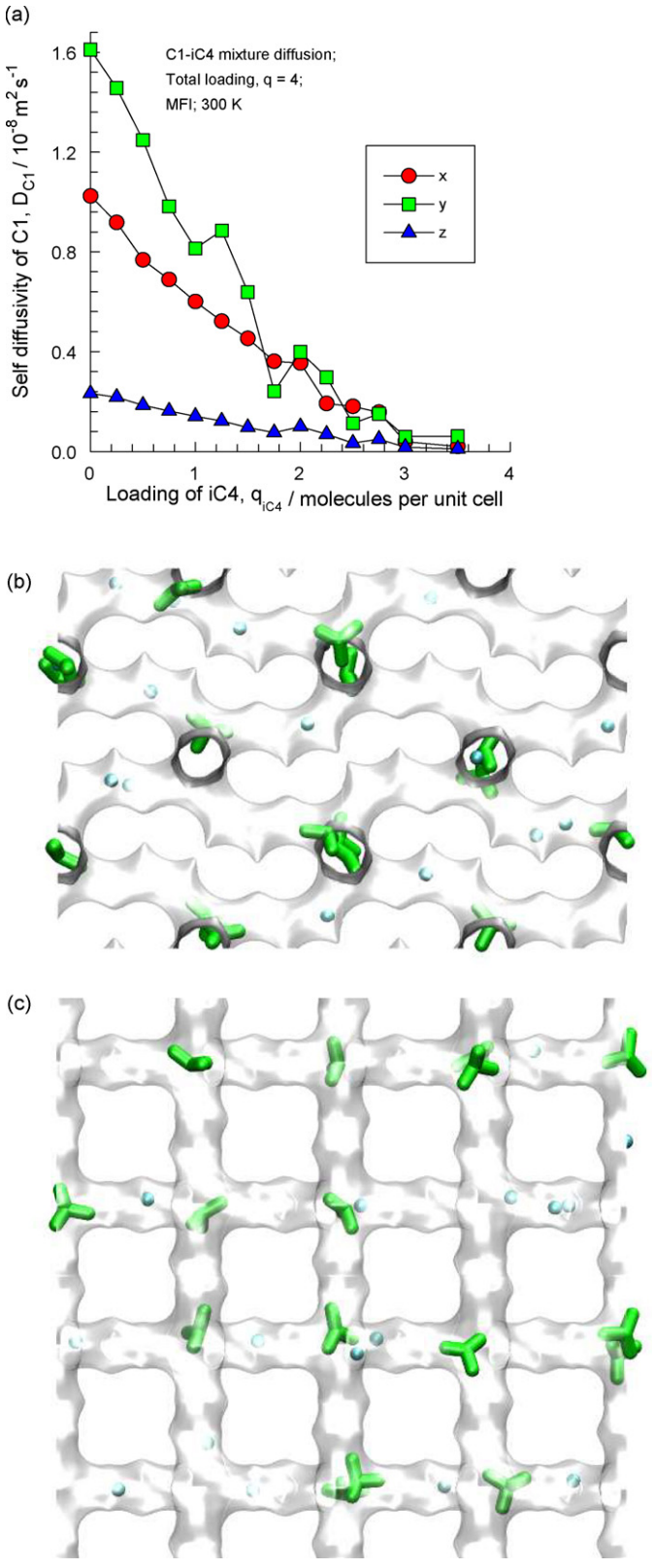

Fig. 4. (a) Self-diffusion coefficients of C1 in C1/*i*C4 mixtures in MFI at 300 K as a function of the loading of *i*C4 in the mixture. Snapshots showing the location of C1 and *i*C4 molecules in MFI, viewed (b) from the top, in the *x*–*z* plane, and (c) from the side, in the *x*–*y* plane. Both views are two unit cells deep. The total loading in the snapshot is $q = 4$, with equal loading of each species.

In MFI zeolite, any tardy species will slow down the diffusion of a more mobile species, and we can ask ourselves the question: what is peculiar about intersection blocking? To answer this question, we have included data for D_{C1} in C1–*n*C4, and C1–*n*C6 mixtures in Fig. 5a. *n*C4 and *n*C6 can adsorb anywhere in the MFI pore space and the reduction of D_{C1} is due to correlation effects [9]; the tardier partner (*n*C6) causes a greater reduction in D_{C1} than *n*C4. The influence of intersection blockage in C1–*i*C4, C1–22DMB and C1–Bz mixtures is more severe as compared to that in C1–*n*C4, and C1–*n*C6 mixture because it does not matter any more which partner molecule (*i*C4, 22DMB, Bz) blocks the intersection, the reduction is the same; C1 molecules need

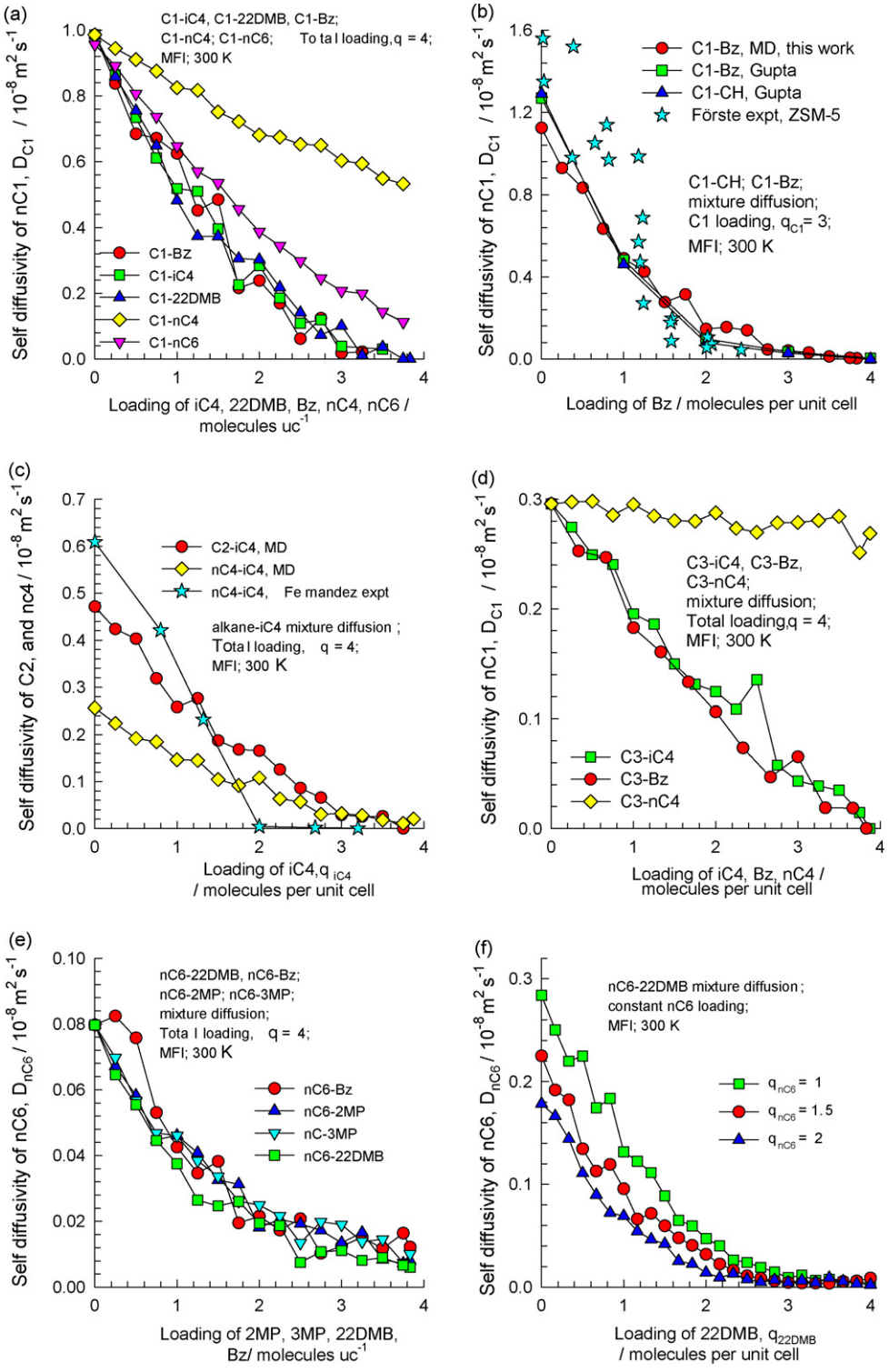

Fig. 5. Self-diffusivities of (a and b) C1, (c) C2, and *n*C4, (d) C3, (e and f) *n*C6 in mixtures with *i*C4, 22DMB, Bz, CH, 3MP or 2MP as a function of the loading of the loading of the partner species.

to by-pass the blocked intersection. For C1–*n*C4 and C1–*n*C6 mixtures, increasing *n*C6 loading has a greater effect on C1 diffusivity than that corresponding to *n*C4. To stress this point further, we compare data for D_{C3} in C3–*i*C4, C3–Bz, and C3–*n*C4 mixtures in Fig. 5d. For C3–*n*C4 mixtures, there is practically no reduction in D_{C3} with increased q_{nC4}. On the other hand, the influence of *i*C4 or Bz is severe, and causes D_{C3} to reduce nearly to zero.

The MD data for D_{nC6} in *n*C6–2MP, *n*C6–3MP, *n*C6–22DMB, and *n*C6–Bz mixtures are presented in Fig. 5e; here the total loading $q = 4$. D_{nC6} shows practically the same dependence on the loading of the partner molecule; intersection blocking by any branched or cyclic hydrocarbon has virtually the same influence on the diffusivity of *n*C6. These results are in qualitative agreement with experimental data for *n*C6–2MP and *n*C6–3MP mixtures [12,13]; a direct comparison with published data is not possible because the loadings inside the zeolite were not measured and the data are presented as a function of gas phase compositions.

Fig. 5f presents MD data for D_{nC6} in *n*C6–22DMB mixtures for which the loading of *n*C6 was held constant at loadings of $q_{nC6} = 1$, 1.5 and 2. The influence of increasing q_{22DMB} is similar in all cases, demonstrating that intersection blocking manifests in a similar fashion irrespective of mixture loading.

The intersection blockage effect can best be appreciated by viewing the animations of the MD simulations [27].

4. Conclusions

Branched or cyclic hydrocarbons such as *i*C4, 2MP, 3MP, 22DMB and Bz adsorb preferentially at the intersections of MFI. This preferential adsorption has two consequences. Firstly, due to the segregated nature of adsorption, the IAST is unable to provide a good quantitative estimate of the component loadings in mixtures. Secondly, the diffusivity of a linear C1–C6 alkane in mixtures with *i*C4, 2MP, 3MP, 22DMB or Bz is severely reduced with increasing loading of its partner molecule; this reduction is due to intersection blocking and is equally deleterious irrespective of which molecule blocks the intersections. Also, the influence of intersection blocking is quantitatively *similar* for all C1–C6 linear alkanes investigated.

There are important consequences of the work reported here in modeling of separation of hydrocarbon mixtures [8,24,28] using an MFI membrane. The strong reduction in the *n*C6 diffusivity due to blockage of the intersections is the one of the causes for the failure of the Maxwell–Stefan (M–S) diffusion equations to provide a good quantitative agreement with experimental data for permeation of *n*C6–3MP mixtures across an MFI membrane, as reported by Zhu et al. [8]. The M–S theory only caters for correlation effects that influence diffusion in hydrocarbon mixtures. Work is in progress to determine ways in which to model intersection blocking using the M–S theory. Another reason for the failure to model the experimental *n*C6–3MP mixture permeation is due to the inability of the IAST to accurately estimate mixture adsorption equilibrium.

Intersection blocking in MFI has consequences in catalysis; it is often observed experimentally that the addition of small amounts of branched hydrocarbons reduces the reactivity of linear hydrocarbons significantly.

Appendix A. Supplementary data

Supplementary data associated with this article can be found, in the online version, at doi:10.1016/j.cej.2007.11.026.

References

[1] H.H. Funke, A.M. Argo, J.L. Falconer, R.D. Noble, Separations of cyclic, branched, and linear hydrocarbon mixtures through silicalite membranes, Ind. Eng. Chem. Res. 36 (1997) 137–143.
[2] C.J. Gump, R.D. Noble, J.L. Falconer, Separation of hexane isomers through nonzeolite pores in ZSM-5 zeolite membranes, Ind. Eng. Chem. Res. 38 (1999) 2775–2781.
[3] J.M. van de Graaf, F. Kapteijn, J.A. Moulijn, Modeling permeation of binary mixtures through zeolite membranes, AIChE J. 45 (1999) 497–511.
[4] M. Arruebo, J.L. Falconer, R.D. Noble, Separation of binary C_5 and C_6 hydrocarbon mixtures through MFI zeolite membranes, J. Membr. Sci. 269 (2006) 171–176.
[5] J. Coronas, R.D. Noble, J.L. Falconer, Separations of C_4 and C_6 isomers in ZSM-5 tubular membranes, Ind. Eng. Chem. Res. 37 (1998) 166–176.
[6] S.K. Gade, V.A. Tuan, C.J. Gump, R.D. Noble, J.L. Falconer, Highly selective separation of *n*-hexane from branched, cyclic and aromatic hydrocarbons using B-ZSM-5 membranes, Chem. Commun. (2001) 601–602.
[7] C.J. Gump, X. Lin, J.L. Falconer, R.D. Noble, Experimental configuration and adsorption effects on the permeation of C_4 isomers through ZSM-5 zeolite membranes, J. Membr. Sci. 173 (2000) 35–52.
[8] W. Zhu, P. Hrabanek, L. Gora, F. Kapteijn, J.C. Jansen, J.A. Moulijn, Modelling of *n*-hexane and 3-methylpentane permeation through a silicalite-1 membrane, Stud. Surf. Sci. Catal. 154 (2004) 1934–1943.
[9] R. Krishna, J.M. van Baten, Diffusion of alkane mixtures in zeolites. Validating the Maxwell–Stefan formulation using MD simulations, J. Phys. Chem. B 109 (2005) 6386–6396.
[10] C. Förste, A. Germanus, J. Kärger, H. Pfeifer, J. Caro, W. Pilz, A. Zikánová, Molecular mobility of methane adsorbed in ZSM-5 containing co-adsorbed benzene, and the location of benzene molecules, J. Chem. Soc., Faraday Trans. 1 83 (1987) 2301–2309.
[11] M. Fernandez, J. Kärger, D. Freude, A. Pampel, J.M. van Baten, R. Krishna, Mixture diffusion in zeolites studied by MAS PFG NMR and molecular simulation, Micropor. Mesopor. Mater. 105 (2007) 124–131.
[12] D. Schuring, A.O. Koriabkina, A.M. de Jong, B. Smit, R.A. van Santen, Adsorption and diffusion of *n*-hexane/2-methylpentane mixtures in zeolite silicalite: experiments and modeling, J. Phys. Chem. B 105 (2001) 7690–7698.
[13] A.O. Koriabkina, A.M. de Jong, D. Schuring, J. van Grondelle, R.A. van Santen, Influence of the acid sites on the intracrystalline diffusion of hexanes and their mixtures within MFI-zeolites, J. Phys. Chem. B 106 (2002) 9559–9566.
[14] T.J.H. Vlugt, W. Zhu, F. Kapteijn, J.A. Moulijn, B. Smit, R. Krishna, Adsorption of linear and branched alkanes in the silicalite-1, J. Am. Chem. Soc. 120 (1998) 5599–5600.
[15] T.J.H. Vlugt, R. Krishna, B. Smit, Molecular simulations of adsorption isotherms for linear and branched alkanes and their mixtures in silicalite, J. Phys. Chem. B 103 (1999) 1102–1118.
[16] R. Krishna, B. Smit, S. Calero, Entropy effects during sorption of alkanes in zeolites, Chem. Soc. Rev. 31 (2002) 185–194.
[17] M. Schenk, S.L. Vidal, T.J.H. Vlugt, B. Smit, R. Krishna, Separation of alkane isomers by exploiting entropy effects during adsorption on silicalite-1: A configurational-bias Monte Carlo simulation study, Langmuir 17 (2001) 1558–1570.
[18] R. Krishna, B. Smit, T.J.H. Vlugt, Sorption-induced diffusion-selective separation of hydrocarbon isomers using silicalite, J. Phys. Chem. A 102 (1998) 7727–7730.

[19] R. Krishna, R. Baur, On the Langmuir–Hinshelwood formulation for zeolite catalysed reactions, Chem. Eng. Sci. 60 (2005) 1155–1166.
[20] A.L. Myers, J.M. Prausnitz, Thermodynamics of mixed gas adsorption, AIChE J. 11 (1965) 121–130.
[21] R. Krishna, S. Calero, B. Smit, Investigation of entropy effects during sorption of mixtures of alkanes in MFI zeolite, Chem. Eng. J. 88 (2002) 81–94.
[22] M. Murthi, R.Q. Snurr, Effects of molecular siting and adsorbent heterogeneity on the ideality of adsorption equilibria, Langmuir 20 (2004) 2489–2497.
[23] R. Krishna, J.M. van Baten, Influence of segregated adsorption on mixture diffusion in DDR zeolite, Chem. Phys. Lett. 446 (2007) 344–349.
[24] R. Krishna, D. Paschek, Separation of hydrocarbon mixtures using zeolite membranes: a modelling approach combining molecular simulations with the Maxwell–Stefan theory, Sep. Purif. Technol. 21 (2000) 111–136.
[25] A. Gupta, R.Q. Snurr, A study of pore blockage in silicalite zeolite using free energy perturbation calculations, J. Phys. Chem. B 109 (2005) 1822–1833.
[26] R. Krishna, J.M. van Baten, Insights into diffusion of gases in zeolites gained from molecular dynamics simulations, Micropor. Mesopor. Mater. 109 (2008) 91–108.
[27] J.M. van Baten, R. Krishna, MD Animations of Diffusion in Zeolites, University of Amsterdam, Amsterdam, October 30, 2007, http://www.science.uva.nl/research/cr/animateMD/.
[28] R. Krishna, R. Baur, Modelling issues in zeolite based separation processes, Sep. Purif. Technol. 33 (2003) 213–254.